Comparison of microbiome profiles different sample types in peri-implantitis patients using 16S RNA sequencing

Kim, Da-Mi

Department of Dentistry

Graduate School

Yonsei University

Comparison of microbiome profiles across different sample types in peri-implantitis patients using 16S rRNA sequencing

Advisor Cha, Jae-Kook

A Dissertation Submitted
to the Department of Dentistry
and the Committee on Graduate School
of Yonsei University in Partial Fulfillment of the
Requirements for the Degree of
Doctor of Dental Science

Kim, Da-Mi

(July) 2025

Comparison of microbiome profiles across different sample types in peri-implantitis patients using 16S rRNA sequencing

This Certifies that the Dissertation
of Kim, Da-Mi is Approved

Committee Chair	**Lee, Jung-Seok**
Committee Member	**Jung, Ui-Won**
Committee Member	**Cha, Jae-Kook**
Committee Member	**Paik, Jeong-Won**
Committee Member	**Park, Jin-Young**

Department of Dentistry
Graduate School
Yonsei University

July 2025

TABLE OF CONTENTS

LIST OF FIGURES

LIST OF TABLES

ABSTRACT

Comparison of microbiome profiles different sample types in peri-implantitis patients using 16S RNA sequencing

Purpose: Numerous studies have applied microbial analyses to peri-implantitis, including for samples collected from various sites. While characteristics of the peri-implantitis microbiome have been identified, differences in sampling methods between studies have not been considered. The present study aimed (1) to characterize microbial similarities among saliva, gingival crevicular fluid (GCF), subgingival plaque (SGP) and inflammatory connective tissue (ICT) in the same subject with peri-implantitis, and (2) to determine the microbial profiles of peri-implantitis sites.

Methods: Saliva, GCF and SGP samples were collected from 18 patients undergoing peri-implantitis surgery, and ICT samples were obtained after flap elevation. The collected samples were analysed using 16S rRNA sequencing.

Results: Sampling sites showed an average bone loss of 6.9 mm, with a deepest probing depth (PD) of 8.3 mm. The alpha diversity did not differ significantly among ICT, GCF and SGP, whereas saliva showed a distinct microbial diversity. Also, the beta diversity analyses indicated that the microbial community structure differed significantly between saliva and the other samples. In taxonomy analyses, the microbial profiles of ICT, GCF and SGP could be clearly discriminated from that of saliva. Saliva showed lower proportions of Bacteroidetes species and higher proportions of Proteobacteria and Actinobacteria species, especially at deep PD sites. Pearson's correlation analyses showed strong similarity between ICT and both GCF and SGP, but not between ICT and saliva. Pathogenic species such as *Porphyromonas gingivalis*, *Tannerella forsythia*, *Treponema denticola*, *Campylobacter rectus*, *Filifactor alocis* and *Porphyromonas endodontalis* were more abundant in ICT than in saliva.

Conclusions: ICT, GCF and SGP shared similar microbial profiles, while saliva exhibited a significantly different profile. The former samples had higher abundances of peri-implant pathogenic species, whereas saliva tended to have lower abundances, and this tendency was more pronounced in deep pockets..

Keywords: Peri-implantitis, 16S rRNA, RNA sequencing, microb

01. INTRODUCTION

Peri-implantitis is primarily driven by microbiome dysbiosis triggering the inflammatory response, leading to the degradation of supporting bone and soft tissues(Berglundh et al., 2018; Hong et al., 2024). Accordingly, identifying of pathogenic microbial changes in peri-implantitis can improve the understanding of disease progression, allowing more-accurate diagnoses and effective treatments. Traditional culture-based methods are inadequate for microbial analyses of peri-implantitis(Mombelli, van Oosten, Schurch, & Land, 1987). However, recent advances in 16S rRNA sequencing have revolutionized the understanding of microbial diversity(Kumar, Mason, Brooker, & O'Brien, 2012; Sanz-Martin et al., 2017). 16S rRNA sequencing analyses the unique ribosomal RNA of microbial species to provide a comprehensive overview of the microbial communities present at different sampling sites(Kim et al., 2022; Mangal et al., 2023).

Saliva, gingival crevicular fluid (GCF) and subgingival plaque (SGP) samples can be collected non-invasively and are rich in biomarkers such as microorganisms, proteins and cytokines. These samples have been widely used for diagnosing diseases and analysing the microbiome(Kim et al., 2022; Kumar et al., 2012; Mangal et al., 2023; Sanz-Martin et al., 2017; Song et al., 2024). However, in a microbial analysis, the bacteria collected from GCF and saliva are those washed out from the SGP, whereas those collected from inflammatory connective tissue (ICT) are those have invaded through the sulcular epithelium.

ICT has been analysed to understand the pathology of periodontal disease, since the inflammatory response is initiated by bacteria that penetrate the host defence of the epithelium in gingival sulcus(Dionigi, Larsson, Carcuac, & Berglundh, 2020; Easter et al., 2024). Because the use of ICT involves obtaining inflamed tissue directly from peri-implantitis sites, this might provide deeper insight into host–pathogen interactions. Pathogenic bacteria such as *Porphyromonas gingivalis* and *Tannerella forsythia* were identified within the ICT surrounding periodontitis lesions(Rajakaruna et al., 2018). Furthermore, recent studies based on single-cell RNA sequencing of keratinocytes from ICT showed cell–bacteria interactions and the regulation of immune responses through cell communication(Easter et al., 2024).

Previous studies that analysed various samples using 16S rRNA sequencing focused on the microbial changes associated with peri-implantiti

s (Jia et al., 2024; Kumar et al., 2012; Philip et al., 2022; Sanz-Martin et al., 2017; Sun et al., 2022; Yu et al., 2024). To the best of our knowledge, no previous studies have compared the microbial profiles of different samples collected from the same subject. Significant differences in microbial profiles according to the sampling methods would make it necessary to consider differences in sampling methods when analyzing the microbiome data of peri-implantitis.

By comparing microbial similarities across different sampling methods from the same lesion, this study aims to guide the selection of clinically relevant and microbiologically representative sampling strategies for microbial analysis of peri-implantitis. Therefore, the aims of the present study were (1) to characterize microbial similarities among saliva, GCF, SGP and ICT in the same subject with peri-implantitis, and (2) to determine the microbial profiles of peri-implantitis sites using 16S rRNA sequencing.

2. MATERIALS AND METHODS

2.1 Patient population

This study enrolled 18 patients receiving peri-implantitis treatment at the Department of Periodontics, Yonsei University Dental Hospital, Seoul, South Korea. These patients had been diagnosed with peri-implantitis (radiographically confirmed peri-implant bone loss ≥ 3 mm and probing depth (PD) ≥ 6 mm, with bleeding and/or suppuration on probing) and scheduled for surgical treatment(Berglundh et al., 2018). The exclusion criteria were a (1) history of surgical treatment for peri-implantitis, (2) untreated periodontitis, (3) smoking, (4) pregnancy, (5) use of drugs affecting periodontal tissues, (6) uncontrolled diabetes mellitus or other systemic diseases, (7) need for antibiotic prophylaxis or (8) history of antibiotic intake in the previous 3 months. Clinical parameter was evaluated with periodontal probe (CP15, Nordent Manufacturing, IL, USA). Periapical x-rays were obtained for radiographic analyses.

If a patient had multiple implants fulfilling the inclusion criteria, the implant with the deepest PD was included in the study. Written informed consent was obtained from all patients after the study had been explained to them. Ethics approval was granted by the Institutional Review Board for Clinical Research at the Dental Hospital of Yonsei University (Approval number: 2-2020-0106). After initial screening, plaque control was performed with a metallic copper-alloy ultrasonic scaler tip (IS TIP, B&L Biotech, Ansan, Korea), and all patients received the same types of toothbrush and toothpaste, along with standardized oral hygiene instructions, until they received surgical treatment.

2.2 Sample collection

Sample collection methods were according to the standard operating procedures (SOP) for the collection, processing, and storage of oral biospecimens at the Korea Oral Biobank Network (Cho et al., 2023). This SOP includes detailed protocols for collection, management, storage of oral biospecimens.

All participants were asked to refrain from eating, rinsing with mouthwash, or toothbrushing for at least 3 hours prior to sample collection to avoid contamination. They were also asked to rinse their mouth with water to remove residual debris and then rest for 5–10 minutes to eliminate any remaining moisture from the rinse. Non-stimulated saliva (5 mL) was collected using the passive drooling method into a sterile 50 mL conical tube (SPL Life Sciences Co., Ltd., Pocheon, Korea) over a period of 5–10 minutes (Figure 1A)(Lee, Chen, Tu, Wu, & Chang, 2018). The GCF was collected by inserting a sterile paper point (#20) into the gingival sulcus(Song et al., 2024). The implant area was carefully isolated and dried with a three-way syringe, and a sterile paper point was gently inserted for 20 seconds into the gingival sulcus at the site with the deepest PD while avoiding contamination from plaque and saliva (Figure 1B). SGP samples were collected using sterile titanium curettes(Gerber, Wenaweser, Heitz-Mayfield, Lang, & Persson, 2006). After removing the implant prosthesis and supragingival biofilm, the peri-implantitis site was isolated using the three-way syringe and cotton pellet. A titanium curette (IMPLG1/2T, Hu-Friedy, IL, USA) was then applied in a single vertical stroke of moderate pressure against the implant surface to collect the SGP (Figure 1C,D). All saliva, GCF, and SGP samples were immediately immersed in RNA stabilizing reagent (RNAlater®, Thermo Fisher Scientific, MA, USA) and stored at −80°C within 10 minutes of collection for subsequent analyses (Cho et al., 2023).

After collecting saliva, GCF and SGP samples, local anaesthesia was administered and a sulcular incision was made for the surgical treatment. A full-thickness flap was gently elevated and rinsed with sterile saline before excising the ICT sample from around the peri-implantitis defects using a sterile titanium curette following an internal bevel incision (Figure 1E, F)(Rajakaruna et al., 2018). ICT samples were immediately placed into sterile saline tubes, and stored at –80°C for subsequent processing. After collecting granulation tissue, surgical peri-implantitis treatment was applied according to the previous protocol (Hong et al., 2024).

2.3 16S rRNA gene sequencing

For the GCF and SGP sample preparation, GCF-soaked paper points and SGP were

added to Lysing Matrix E tubes (MP Biomedicals, CA, USA), to which 978 μL of sodium phosphate buffer and 122 μL of Matrix T buffer (MP Biomedicals) were added. The saliva samples were prepared by adding 800 μL to Lysing Matrix E tubes, followed by 200 μL of sodium phosphate buffer and 122 μL of Matrix T buffer. For ICT sample preparation, 50 mg of ICT samples were homogenized using liquid nitrogen and then added to 978 μL of sodium phosphate buffer and 122 μL of Matrix T buffer. All samples were homogenized using liquid nitrogen. After preparation, all samples were disrupted using the FastPrep instrument for 40 seconds at a speed setting of 6 meters/second to disrupt the cell walls and release nucleic acids. Total bacteria genomic DNA was extracted from all samples using the FastDNA Spin kit (MP Biomedicals). Beads were added, and samples were disrupted for 40 seconds using the TissueLyser device (Qiagen, Hilden, Germany). PCR amplification was performed using the following fusion primers targeting regions V3 to V4 of the 16S rRNA gene with the extracted DNA: 341F, 5'-AATGATACGGCGACCACCGAGATCTACAC-XXXXXXXX-TCGTCGGCAGCGTCAGATGTGTATAAGAGACAG-CCTACGGGNGGCWGCAG-3'; and 805R, (5'- CAAGCAGAAGACGGCATACGAGAT-XXXXXXXXGTCTCGTGGGCTCGG-AGATGTGTATAAGAGACAG-GACTACHVGGGTATCTAATCC-3'. The fusion primers were constructed in the following order: P5 (P7) graft binding, i5 (i7) index, Nextera consensus, sequencing adaptor and target region sequence. The PCR conditions were an initial denaturation at 95°C for 3 minutes; followed by 25 cycles of denaturation at 95°C for 30 seconds, primer annealing at 55°C for 30 seconds and extension at 72°C for 30 seconds; with a final extension at 72°C for 5 minutes. The sample DNA was analysed by sequencing the V3-to-V4 hypervariable region of the 16S rRNA gene using the MiSeq platform (Illumina, CA, USA).

2.4 Raw data preparation and statistical analyses

Raw paired-end Illumina sequences were processed using the dada2 pipeline (version 1.32.0) as described previously(Callahan et al., 2016). In brief, primers were trimmed and filtered using the filterAndTrim function to remove those with more than 4 (forward) and

6 (reverse) expected errors based on the quality scores, and truncated after 280 (forward) and 260 (reverse) base pairs. The dada2 algorithm was applied to infer exact amplicon sequence variants (ASVs) from the processed sequences while filtering chimeras. Taxonomy was assigned to the ASVs using a naive Bayesian classifier method against the eHOMD (expanded Human Oral Microbiome Database) (version 15.1) with a minimum bootstrap confidence of 50. An ASV table was constructed by recording the number of times each ASV was observed in each sample.

The ASV table, sample data and taxonomy table were imported into the R environment as phyloseq objects (version 1.48.0)(McMurdie & Holmes, 2013). Additional sample data categories were added to the phyloseq sample data table. ASVs with no phylum assigned were filtered out and agglomerated over the species level. Alpha and beta diversity metrics were calculated on the filtered ASV table using the estimate_richness and ordinate functions in the phyloseq package. All plots were generated using the ggplot2 package (version 3.5.1). Heat maps were drawn using the ComplexHeatmap package (version 2.20.0)(Gu, 2022). All statistical analyses and visualizations were performed in the R (version 4.4.1) and RStudio environments.

This study was designed as an exploratory, within-subject comparison of microbiome profiles across different sampling methods from peri-implantitis lesions. Therefore, no formal sample size calculation was performed. A total of 18 patients were enrolled, each contributing four sample types. This sample size was considered appropriate for non-parametric paired statistical analyses

Samples from the same subject were paired for the statistical analyses. The microbial community richness and diversity (alpha diversity) of the samples were quantified using the Shannon index. The microbiome characteristics (beta diversity) were compared using principal-coordinate analysis. Scatter plots were generated to compare the microbial abundance ranks between different samples, with the *x*- and *y*-axes representing the ranks of a particular species in ICT and its paired sample, respectively, from the same subject. Correlations between the samples were assessed by comparing Spearman's correlation coefficients of the ICT and the other samples using Fisher's Z test. The abundance ranks and relative abundances of seven known pathogenic bacterial species related to peri-

implantitis (*P. gingivalis*, *T. forsythia*, *Treponema denticola*, *Campylobacter rectus*, *Filifactor alocis*, *Fusobacterium nucleatum* and *Porphyromonas endodontalis*) were pairwise ranked using the Friedman test (Belibasakis & Manoil, 2021; Jia et al., 2024; Sanz-Martin et al., 2017; Yu et al., 2024). Subgroup analyses were applied based on PD: moderate-PD group (PD = 6–8 mm) and deep-PD group (PD ≥ 9 mm) (Farina, Filippi, Brazzioli, Tomasi, & Trombelli, 2017).

3.RESULTS

3.1 Demographic and clinical characteristics of the subjects

The demographic and clinical characteristics of the subjects are summarized in Tables 1. None of the subjects were smokers. As shown in the table, implants affected by peri-implantitis showed an average bone loss of 6.9 mm. The deepest PD site, from which both GCF and SGP were collected, had an average PD of 8.3 mm.

3.2 Microbial diversity similarities among saliva, GCF, SGP and ICT

The Shannon indices did not differ significantly among paired GCF, SGP and ICT samples, while they did between the paired saliva samples and the other sample types ($p < 0.05$) (Figure 2A). The Shannon indices of saliva samples differed significantly from those of paired ICT and GCF samples in the deep-PD group, while there were no significant intersample differences in the moderate-PD group. The results of the beta diversity analyses are shown in Figure 2B. The community structure of saliva was clearly distinct from those of the other samples in both study groups.

3.3 Taxonomy profiles of peri-implantitis sites and similarities of taxonomy profiles among the collection methods

In overall microbial profiles, saliva exhibited distinct microbial profiles, with a lower proportion of Bacteroidetes species and higher proportions of Proteobacteria and Actinobacteria species (Figure 3A). These differences were larger in the deep-PD group (Figure 3B). In addition, at the genus level, ICT and SGP samples showed high relative abundances of peri-implantitis-associated pathogenic genera such as Porphyromonas, Treponema, and Tannerella, while GCF samples exhibited similar compositional trends. In contrast, saliva samples were characterized by a more even distribution of commensal genera, including Streptococcus and Veillonella. (Figure 3C).

Scatter plots comparing the abundance ranks of ICT samples with their paired samples revealed strong positive correlations for ICT vs GCF and ICT vs SGP, with no significant difference in Pearson correlation coefficients (Figure 4A, Supplementary Figure 2). However, the correlation was weak for ICT vs saliva, and the Pearson correlation coefficient was significantly lower for ICT vs saliva than for ICT vs GCF and ICT vs SGP (Figure 4B).

3.4 Abundance ranks of peri-implantitis pathogenic species

P. gingivalis, *T. forsythia*, *T. denticola*, *C. rectus*, *F. alocis* and *P. endodontalis* exhibited significantly higher abundance ranks in ICT than in saliva (Figure 5A). In subgroup analyses this trend was observed in both the deep- and moderate-PD groups (Figure 5B). However, in the deep-PD group, *P. gingivalis* had a high abundance rank among all paired samples, with no significant differences among them.

The relative abundances of peri-implantitis pathogenic species are presented in Figure 6. These differed significantly with the sample type for three red-complex species (Figure 6A), being markedly lower for *P. gingivalis* in saliva, significantly higher for *T. forsythia* in ICT, and significantly higher for *T. denticola* in ICT than in saliva and SGP. Subgroup analyses of the deep- and moderate-PD groups revealed that the relative abundance of *P. gingivalis* was significantly lower in saliva, while *T. forsythia* and *T. denticola* were more abundant in ICT than saliva in both groups, with these differences being particularly large in the deep-PD group (Figure 6B).

4. DISCUSSION

This study investigated the microbial profiles of peri-implantitis sites using 16S rRNA sequencing at different sampling sites. This revealed similar microbial profiles for ICT, GCF and SGP, while saliva exhibited significantly different profiles, with the difference being larger at sites with deeper PDs. The analyses of peri-implantitis pathogenic species showed a similar pattern, with ICT, GCF and SGP displaying higher abundances of these species, and saliva tending to have lower abundances. Notably, *T. forsythia* and *T. denticola* exhibited significantly higher relative abundance in ICT from deep PD sites relative to saliva.

The oral cavity is a complex ecosystem with various niches used for microbiome analyses(Zaura, Pappalardo, Buijs, Volgenant, & Brandt, 2021). The selected niche-specific samples vary with the objectives of a study. For example, Kim et al. analysed SGP, supragingival plaque and saliva in patients with periodontitis, and found that saliva had the highest diversity and a broader range of species, though generally with lower abundances(Kim et al., 2022). Similarly, Zhang et al. found that saliva from oral cancer patients displayed higher diversity and significantly different microbial communities relative to dental plaque samples(Zhang et al., 2024). Consistent with these previous studies, we found that the microbial communities of saliva differed significantly from those of ICT, GCF and SGP, with higher diversity and a wider range of low-abundance species. These observations may be due the role that saliva has in transporting microorganisms from various microbial niches in the oral cavity, such as the tongue and buccal mucosa(Zhang et al., 2024). Therefore, while sampling saliva is convenient, this may underestimate site-specific microbial changes at peri-implantitis sites, showing lower abundances of pathogenic species associated with peri-implantitis.

The microbial differences between saliva and the other samples in this study were larger in patients with deep PD (PD ≥ 9 mm). Previous investigations of SGP samples obtained

from periodontitis patients also identified significant differences in microbial profiles between deep and shallow PD sites. These differences were primarily due to higher abundances of pathogenic species such as *P. gingivalis*, *T. denticola*, *T. forsythia* and *F. alocis* at deep PD (PD ≥ 7 mm) sites(Pérez-Chaparro et al., 2018). While the PD threshold for deep PD in our study (≥9 mm) differs from that used in the previous study on periodontitis (PD ≥ 7 mm), the overall trend remains consistent: deeper PD is associated with increased presence of pathogenic species. Additionally, since peri-implantitis and periodontitis differ in tissue characteristic and disease progression, direct comparisons of numerical PD cutoffs across studies should be made with caution.

The environment at the base of the periodontal pocket is anaerobic and characterized by active tissue destruction due to inflammation. This differs markedly from the overall environment of the oral cavity, and so microbiome data derived from saliva might not accurately reflect critical aspects of disease progression. Furthermore, saliva samples are influenced more than site-specific samples by general factors unrelated to diseases that can significantly impact the saliva microbiome, such as sociodemographic characteristics and antibiotic use(Karadayı et al., 2024; Mangal et al., 2023; Renson et al., 2019). Caution is therefore required when interpreting the results of microbial analyses based on saliva samples obtained in peri-implantitis.

Peri-implantitis is considered a plaque-induced inflammatory condition associated with dysbiosis of the peri-implant microbiome. This dysbiosis typically involves increased species richness in the submucosal microbiome, accompanied by significant increases in pathogenic microorganisms from the red and orange complexes(Belibasakis & Manoil, 2021). These changes are evident in 16S rRNA sequencing data from GCF and SGP samples, where, following peri-implantitis treatment, the microbiome of the affected site shifts towards a microbial profile with fewer red-complex bacteria and reduced diversity(Philip et al., 2022; Sun et al., 2022). However, few studies have analysed the microbial profile of peri-implantitis lesions using ICT. Unlike GCF and plaque samples, ICT is likely to contain bacteria that can invade the sulcular epithelium and evade host defense mechanisms (Park et al., 2024). Nonetheless, the ICT samples obtained in the

present study showed a microbial profile similar to those of the SGP and GCF samples.

Host tissue is included in collected ICT samples, which allows for the analysis of host–microbe interactions through human cDNA and single-cell RNA sequencing, thereby providing insights into the molecular mechanisms of host defense mechanisms. A previous investigation of ICT from peri-implantitis sites revealed disease mechanisms via transcriptome profiling (Becker et al., 2014). Additionally, single-cell RNA sequencing of ICT enables the analysis of inflammatory modulation among cellular components involved in periodontal inflammation(Easter et al., 2024). Therefore, ICT-based microbiome analysis offers a methodological advantage in interpreting microbiome alterations in relation to the host's immune response(Ganesan et al., 2022). Selecting appropriate sampling methods is essential for accurately characterizing the microbial environment at diseased peri-implant sites. As ICT, GCF, and SGP showed similar microbial signatures, while saliva displayed a distinct profile, sampling strategies for peri-implant microbiome studies and diagnostics should prioritize tissue- or sulcus-based sources. Future studies integrating host transcriptomics or proteomics with microbial profiling of ICT may further elucidate the mechanisms of peri-implantitis and facilitate more targeted host-tailored interventions.

Although host transcriptome analyses were not conducted in the present study, the use of ICT as a sampling source inherently includes host tissue components. This provides a unique opportunity for future multi-omics studies, such as single-cell RNA sequencing or bulk transcriptomic profiling, to investigate host immune responses in conjunction with microbial dynamics. By enabling such integrative approaches, ICT-based sampling can bridge the gap between microbial composition and clinical pathogenesis of peri-implantitis.

The relative abundances of *T. denticola* and *T. forsythia* were significantly higher in ICT from deep PD sites than in saliva, while that of *P. gingivalis* was significantly lower in saliva than in the other sample types. A previous study that applied DNA–DNA hybridization of SGP identified these three bacteria associated with the severity of periodontitis as the red complex(Socransky, Haffajee, Cugini, Smith, & Kent, 1998).

Studies applying 16S rRNA sequencing to SGP samples have further confirmed that the red complex plays a pivotal role in the progression of peri-implantitis(Jia et al., 2024; Sun et al., 2022; Yu et al., 2024). The red complex contributes to periodontitis by producing enzymes that destroy host tissue and by modulating the immune system, which allows these pathogens to invade tissue(Rajakaruna et al., 2018; Schäffer & Andrukhov, 2024). In particular, *T. forsythia* is capable of invading oral epithelial cells, a process facilitated by the activation of phosphatidylinositol 3-kinase (PI3K) through its BspA protein, among other mechanisms (Mishima & Sharma, 2011). Additionally, T. forsythia is known to adhere to and invade epithelial cells through a mechanism mediated by NanH sialidase (Frey et al., 2018). T. forsythia's potential to influence oral antimicrobial defense through protease-mediated degradation and interactions with other bacteria highlights its significance in periodontal disease pathogenesis (Schäffer & Andrukhov, 2024). In this study, since ICT only contains pathogenic species capable of invading tissue from the oral cavity, the higher relative abundance of the red complex probably reflects the invasive nature of these pathogens.

This study had several limitations. First, the overall sample was small. The oral microbiome exhibits significant interindividual variability, and also fluctuates over time in the same individual(Arredondo et al., 2023; Mangal et al., 2023). Given the vast amount of information provided by 16S rRNA sequencing, larger samples may be necessary for disease-related changes to be distinguished statistically from individual differences. Therefore, while this study identified differences in the microbiome between sampling sites within the same individual, the smallness of the samples reduces the ability to generalize the findings and fully analyse the microbial profile of peri-implantitis. Second, despite efforts to prevent cross-contamination, potential mixing of GCF and SGP during sample collection cannot be completely ruled out, which may have influenced the microbial profiles. Lastly, missing records meant that the implant type was not standardized. Titanium particles generated by corrosion in an inflammatory environment can alter the microbiome, and such factors may vary depending on the type of implant used(Kotsakis & Olmedo, 2021). This variability in implant materials and design could introduce additional confounding factors that were not controlled for in this study.

In conclusion, this study demonstrated that ICT, GCF, and SGP from peri-implantitis sites shared similar microbial profiles, whereas saliva exhibited a distinct microbial community structure, particularly at sites with deeper PD (PD ≥ 9 mm). Moreover, ICT, GCF, and SGP showed higher abundances of peri-implantitis-associated pathogenic species compared to saliva. Although saliva sampling is convenient and non-invasive, it may fail to capture site-specific pathogenic shifts that are more accurately reflected in localized samples such as ICT, GCF, or SGP. These findings underscore the need for carefully selected sampling strategies in both clinical and research settings to ensure precise characterization of microbial dysbiosis in peri-implantitis. ICT sampling, in particular, may provide valuable insights into the host–microbe interface, facilitating the exploration of disease mechanisms through integrated microbial and host-response analyses. Future studies involving larger cohorts and standardized implant systems are warranted to validate and expand upon the present findings.

References

Arredondo, A., Àlvarez, G., Isabal, S., Teughels, W., Laleman, I., Contreras, M. J., . . . León, R. (2023). Comparative 16S rRNA gene sequencing study of subgingival microbiota of healthy subjects and patients with periodontitis from four different countries. *J Clin Periodontol, 50*(9), 1176-1187. doi:10.1111/jcpe.13827

Becker, S. T., Beck-Broichsitter, B. E., Graetz, C., Dörfer, C. E., Wiltfang, J., & Häsler, R. (2014). Peri-implantitis versus periodontitis: functional differences indicated by transcriptome profiling. *Clin Implant Dent Relat Res, 16*(3), 401-411. doi:10.1111/cid.12001

Belibasakis, G. N., & Manoil, D. (2021). Microbial Community-Driven Etiopathogenesis of Peri-Implantitis. *J Dent Res, 100*(1), 21-28. doi:10.1177/0022034520949851

Berglundh, T., Armitage, G., Araujo, M. G., Avila-Ortiz, G., Blanco, J., Camargo, P. M., . . . Zitzmann, N. (2018). Peri-implant diseases and conditions: Consensus report of workgroup 4 of the 2017 World Workshop on the Classification of Periodontal and Peri-Implant Diseases and Conditions. *J Periodontol, 89 Suppl 1*, S313-s318. doi:10.1002/jper.17-0739

Callahan, B. J., McMurdie, P. J., Rosen, M. J., Han, A. W., Johnson, A. J., & Holmes, S. P. (2016). DADA2: High-resolution sample inference from Illumina amplicon data. *Nat Methods, 13*(7), 581-583. doi:10.1038/nmeth.3869

Cho, Y. D., Cho, E. S., Song, J. S., Kim, Y. Y., Hwang, I., & Kim, S. Y. (2023). Standard operating procedures for the collection, processing, and storage of oral biospecimens at the Korea Oral Biobank Network. *Journal of Periodontal and Implant Science, 53*(5), 336-346. doi:10.5051/jpis.2203680184

Dionigi, C., Larsson, L., Carcuac, O., & Berglundh, T. (2020). Cellular expression of DNA damage/repair and reactive oxygen/nitrogen species in human periodontitis and peri-implantitis lesions. *J Clin Periodontol, 47*(12), 1466-1475. doi:10.1111/jcpe.13370

Easter, Q. T., Fernandes Matuck, B., Beldorati Stark, G., Worth, C. L., Predeus, A. V., Fremin, B., . . . Byrd, K. M. (2024). Single-cell and spatially resolved interactomics of tooth-associated keratinocytes in periodontitis. *Nat Commun, 15*(1), 5016.

doi:10.1038/s41467-024-49037-y

Farina, R., Filippi, M., Brazzioli, J., Tomasi, C., & Trombelli, L. (2017). Bleeding on probing around dental implants: a retrospective study of associated factors. *Journal of clinical periodontology, 44*(1), 115-122.

Frey, A. M., Satur, M. J., Phansopa, C., Parker, J. L., Bradshaw, D., Pratten, J., & Stafford, G. P. (2018). Evidence for a carbohydrate-binding module (CBM) of Tannerella forsythia NanH sialidase, key to interactions at the host–pathogen interface. *Biochemical Journal, 475*(6), 1159-1176.

Ganesan, S. M., Dabdoub, S. M., Nagaraja, H. N., Mariotti, A. J., Ludden, C. W., & Kumar, P. S. (2022). Biome-microbiome interactions in peri-implantitis: A pilot investigation. *J Periodontol, 93*(6), 814-823. doi:10.1002/jper.21-0423

Gerber, J., Wenaweser, D., Heitz-Mayfield, L., Lang, N. P., & Persson, G. R. (2006). Comparison of bacterial plaque samples from titanium implant and tooth surfaces by different methods. *Clin Oral Implants Res, 17*(1), 1-7. doi:10.1111/j.1600-0501.2005.01197.x

Gu, Z. (2022). Complex heatmap visualization. *Imeta, 1*(3), e43. doi:10.1002/imt2.43

Hong, I., Koo, K. T., Oh, S. Y., Park, H. W., Sanz-Martin, I., & Cha, J. K. (2024). Comprehensive treatment protocol for peri-implantitis: an up-to date narrative review of the literature. *J Periodontal Implant Sci, 54*(5), 295-308. doi:10.5051/jpis.2303360168

Jia, P., Guo, X., Ye, J., Lu, H., Yang, J., & Hou, J. (2024). Microbiome of diseased and healthy implants-a comprehensive microbial data analysis. *Front Cell Infect Microbiol, 14*, 1445751. doi:10.3389/fcimb.2024.1445751

Karadayı, B., Karaismailoğlu, B., Karadayı, S., Arslan, A., Gözen, E. D., & Özbek, T. (2024). The uselessness of using salivary microbiota in forensic identification purposes of a person with recent antibiotic use. *Leg Med (Tokyo), 69*, 102338. doi:10.1016/j.legalmed.2023.102338

Kim, Y. T., Jeong, J., Mun, S., Yun, K., Han, K., & Jeong, S. N. (2022). Comparison of the oral microbial composition between healthy individuals and periodontitis patients in different oral sampling sites using 16S metagenome profiling. *J Periodontal Implant Sci, 52*(5), 394-410. doi:10.5051/jpis.2200680034

Kotsakis, G. A., & Olmedo, D. G. (2021). Peri-implantitis is not periodontitis: Scientific discoveries shed light on microbiome-biomaterial interactions that may determine disease phenotype. *Periodontol 2000, 86*(1), 231-240. doi:10.1111/prd.12372

Kumar, P. S., Mason, M. R., Brooker, M. R., & O'Brien, K. (2012). Pyrosequencing reveals unique microbial signatures associated with healthy and failing dental implants. *J Clin Periodontol, 39*(5), 425-433. doi:10.1111/j.1600-051X.2012.01856.x

Lee, C. H., Chen, Y. W., Tu, Y. K., Wu, Y. C., & Chang, P. C. (2018). The potential of salivary biomarkers for predicting the sensitivity and monitoring the response to nonsurgical periodontal therapy: A preliminary assessment. *J Periodontal Res, 53*(4), 545-554. doi:10.1111/jre.12544

Mangal, U., Noh, K., Lee, S., Cha, J. K., Song, J. S., Cha, J. Y., . . . Choi, S. H. (2023). Multistability and hysteresis in states of oral microbiota: Is it impacting the dental clinical cohort studies? *J Periodontal Res, 58*(2), 381-391. doi:10.1111/jre.13098

McMurdie, P. J., & Holmes, S. (2013). phyloseq: an R package for reproducible interactive analysis and graphics of microbiome census data. *PLoS One, 8*(4), e61217. doi:10.1371/journal.pone.0061217

Mishima, E., & Sharma, A. (2011). Tannerella forsythia invasion in oral epithelial cells requires phosphoinositide 3-kinase activation and clathrin-mediated endocytosis. *Microbiology, 157*(8), 2382-2391.

Mombelli, A., van Oosten, M. A., Schurch, E., Jr., & Land, N. P. (1987). The microbiota associated with successful or failing osseointegrated titanium implants. *Oral Microbiol Immunol, 2*(4), 145-151. doi:10.1111/j.1399-302x.1987.tb00298.x

Park, J. Y., Han, D., Park, Y., Cho, E. S., In Yook, J., & Lee, J. S. (2024). Intracellular infection of Cutibacterium acnes in macrophages of extensive peri-implantitis lesions: A clinical case series. *Clin Implant Dent Relat Res, 26*(6), 1126-1134. doi:10.1111/cid.13367

Pérez-Chaparro, P. J., McCulloch, J. A., Mamizuka, E. M., Moraes, A., Faveri, M., Figueiredo, L. C., . . . Feres, M. (2018). Do different probing depths exhibit striking differences in microbial profiles? *J Clin Periodontol, 45*(1), 26-37. doi:10.1111/jcpe.12811

Philip, J., Buijs, M. J., Pappalardo, V. Y., Crielaard, W., Brandt, B. W., & Zaura, E. (2022). The microbiome of dental and peri-implant subgingival plaque during peri-implant mucositis therapy: A randomized clinical trial. *J Clin Periodontol, 49*(1), 28-38. doi:10.1111/jcpe.13566

Rajakaruna, G. A., Negi, M., Uchida, K., Sekine, M., Furukawa, A., Ito, T., . . . Eishi, Y. (2018). Localization and density of Porphyromonas gingivalis and Tannerella forsythia in gingival and subgingival granulation tissues affected by chronic or aggressive periodontitis. *Sci Rep, 8*(1), 9507. doi:10.1038/s41598-018-27766-7

Renson, A., Jones, H. E., Beghini, F., Segata, N., Zolnik, C. P., Usyk, M., . . . Dowd, J. B. (2019). Sociodemographic variation in the oral microbiome. *Ann Epidemiol, 35*, 73-80.e72. doi:10.1016/j.annepidem.2019.03.006

Sanz-Martin, I., Doolittle-Hall, J., Teles, R. P., Patel, M., Belibasakis, G. N., Hämmerle, C. H. F., . . . Teles, F. R. F. (2017). Exploring the microbiome of healthy and diseased peri-implant sites using Illumina sequencing. *J Clin Periodontol, 44*(12), 1274-1284. doi:10.1111/jcpe.12788

Schäffer, C., & Andrukhov, O. (2024). The intriguing strategies of Tannerella forsythia's host interaction. *Front Oral Health, 5*, 1434217. doi:10.3389/froh.2024.1434217

Socransky, S. S., Haffajee, A. D., Cugini, M. A., Smith, C., & Kent, R. L., Jr. (1998). Microbial complexes in subgingival plaque. *J Clin Periodontol, 25*(2), 134-144. doi:10.1111/j.1600-051x.1998.tb02419.x

Song, L., Lu, H., Jiang, J., Xu, A., Huang, Y., Huang, J. P., . . . He, F. (2024). Metabolic profiling of peri-implant crevicular fluid in peri-implantitis. *Clin Oral Implants Res, 35*(7), 719-728. doi:10.1111/clr.14270

Sun, F., Wei, Y., Li, S., Nie, Y., Wang, C., & Hu, W. (2022). Shift in the submucosal microbiome of diseased peri-implant sites after non-surgical mechanical debridement treatment. *Front Cell Infect Microbiol, 12*, 1091938. doi:10.3389/fcimb.2022.1091938

Yu, P. S., Tu, C. C., Wara-Aswapati, N., Wang, C. Y., Tu, Y. K., Hou, H. H., . . . Chen, Y. W. (2024). Microbiome of periodontitis and peri-implantitis before and after therapy: Long-read 16S rRNA gene amplicon sequencing. *J Periodontal Res, 59*(4), 657-668. doi:10.1111/jre.13269

Zaura, E., Pappalardo, V. Y., Buijs, M. J., Volgenant, C. M. C., & Brandt, B. W. (2021). Optimizing the quality of clinical studies on oral microbiome: A practical guide for planning, performing, and reporting. *Periodontol 2000, 85*(1), 210-236. doi:10.1111/prd.12359

Zhang, M., Zhao, Y., Umar, A., Zhang, H., Yang, L., Huang, J., . . . Yu, Z. (2024). Comparative analysis of microbial composition and functional characteristics in dental plaque and saliva of oral cancer patients. *BMC Oral Health, 24*(1), 411. doi:10.1186/s12903-024-04181-1

TABLES

Table 1. Demographic and clinical characteristics of the subjects

Parameters	Peri-implantitis (n=18)
Patient age (median, range)	65 [49, 79]
Gender (M/F)	5/13
HTN (Y/N)	5/13
DM (Y/N)	5/13
Smoking (Y/N)	0/18
Periodontitis diagnosis (Stage II/III/IV)	2/11/5
Radiographic bone loss (median, range)	6.685 [2.79, 10.45]
PD (median, range)	6 [3, 12]
PD (at deep site sampled) (median, range)	7.5 [6, 12]
Implant type (tissue level/bone level)	1/17
Implant prosthesis type (screw/cement)	9/9
Location of implant (maxilla/mandible)	7/11
Location of implant (posterior/anterior)	18/0

FIGURE LEGEND

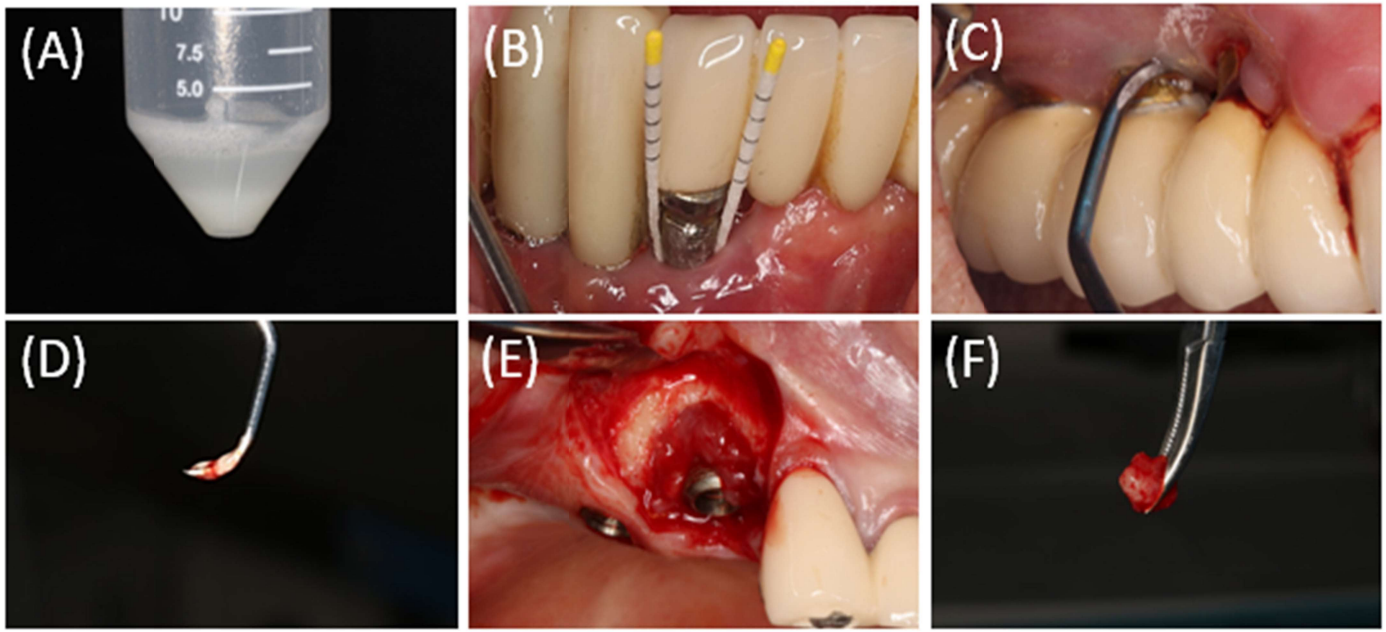

Figure 1. Representative sample collection from a peri-implantitis patient.

(A) Saliva sample. (B) Gingival crevicular fluid (GCF) sampling. (C,D) Subgingival plaque (SGP) sample. (E,F) Inflammaory connective tissue (ICT) sample.

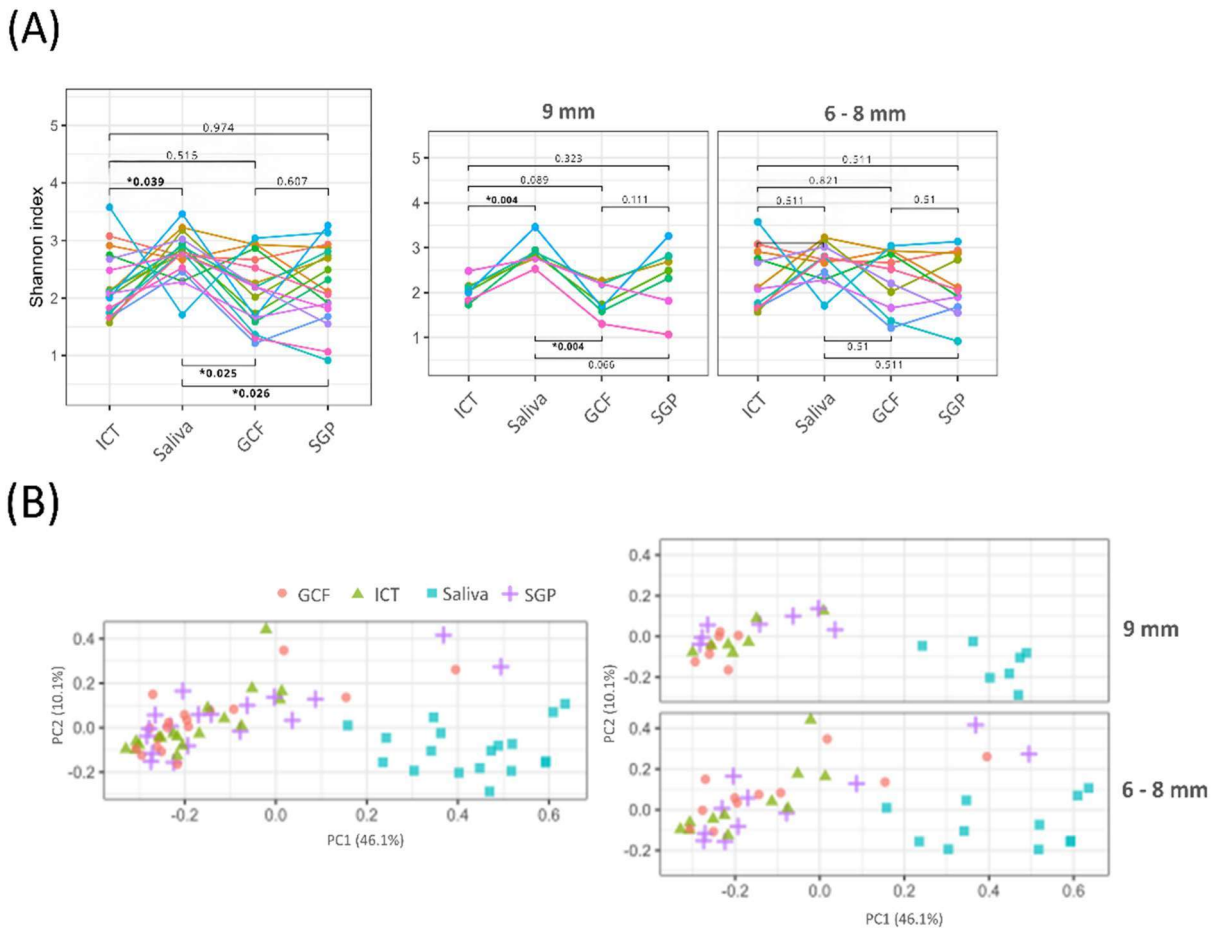

Figure 2. Comparison of microbial diversity among ICT, saliva, GCF and SGP.

(A) Alpha diversity quantified using the Shannon index, which in the saliva samples differed significantly from the other three samples overall, and from the ICT and GCF samples in the deep-PD (probing depth) group. (B) Principal-coordinate analysis plot comparing beta diversities. Saliva showed differences relative to the other samples in both study groups. *, $p < 0.05$.

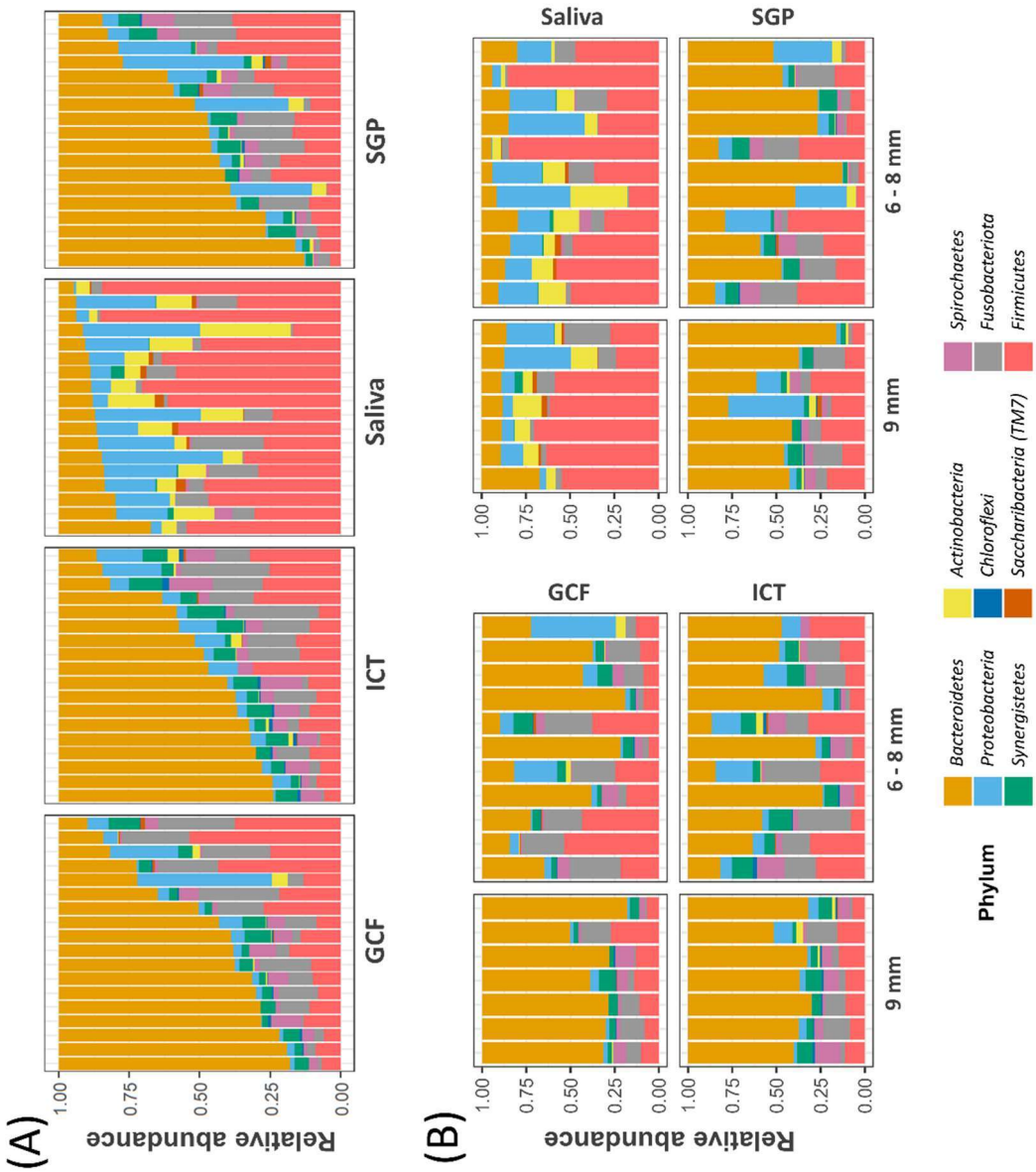

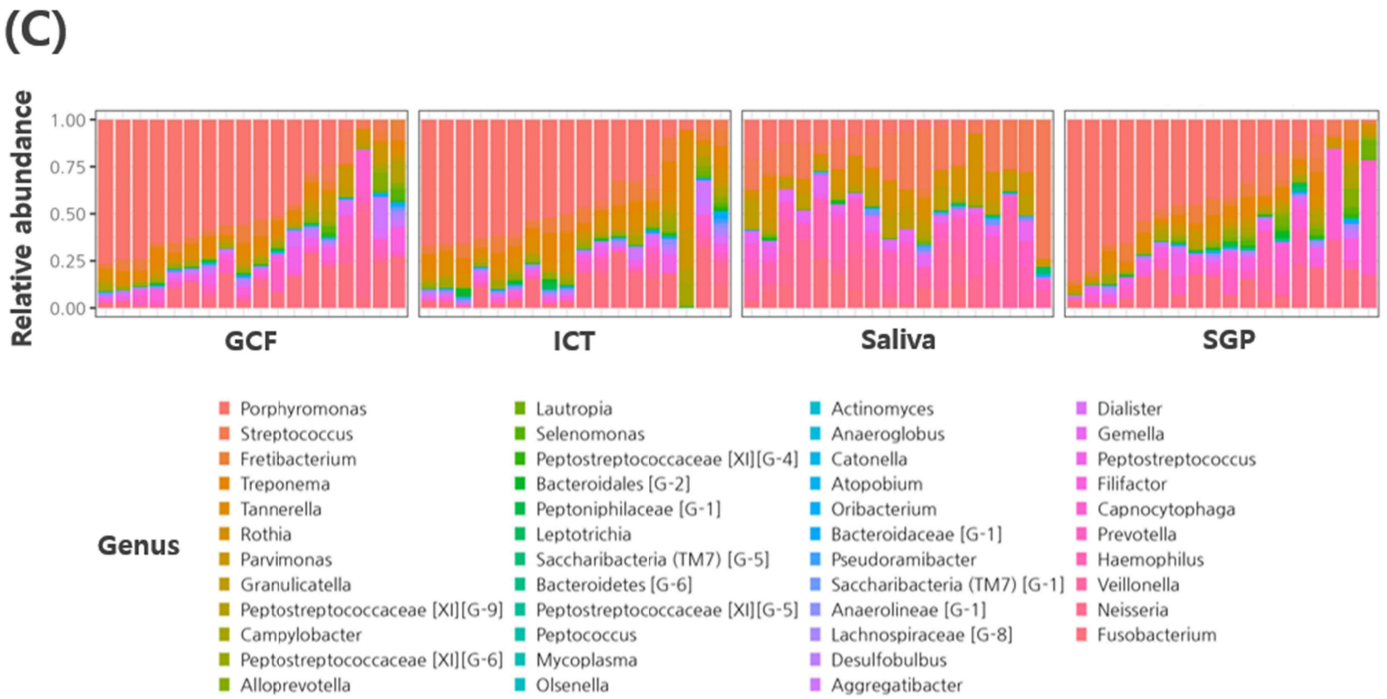

Figure 3. Taxonomy microbial profiles of peri-implantitis ICT, saliva, GCF and SGP.

(A) The overall microbial profile of saliva differed markedly from those of the other samples. (B) Differences in the taxonomy microbial profiles between saliva and the other samples were larger in the deep-PD group. (C) At the genus level, ICT, GCF, and SGP showed similar profiles, whereas saliva was enriched with commensal genera such as Streptococcus and Veillonella.

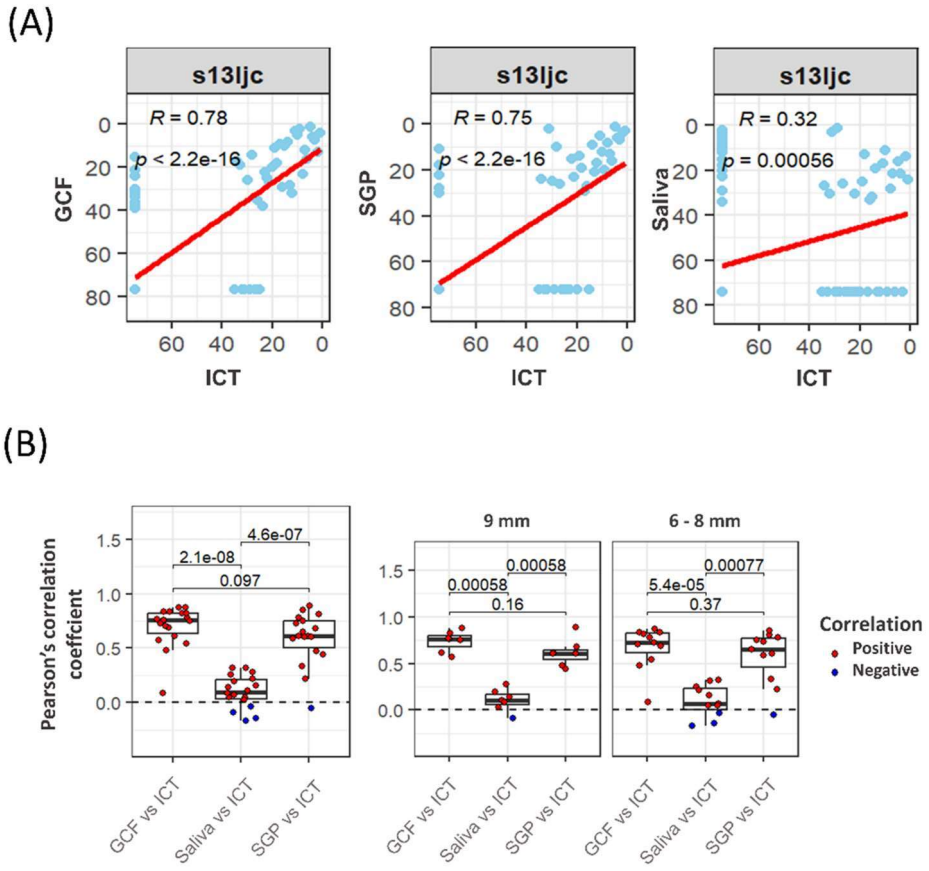

Figure 4. Rank-rank correlations among microbial species abundances.

(A) Scatter plots comparing the ranks of microbial species between ICT and other collection sites (GCF, SGP and saliva) in a single exemplar patient (patient s13ljc; scatter plots of all patients are presented in Supplementary Figure 1). (B) Box plots of Pearson's correlation coefficients for all patients.

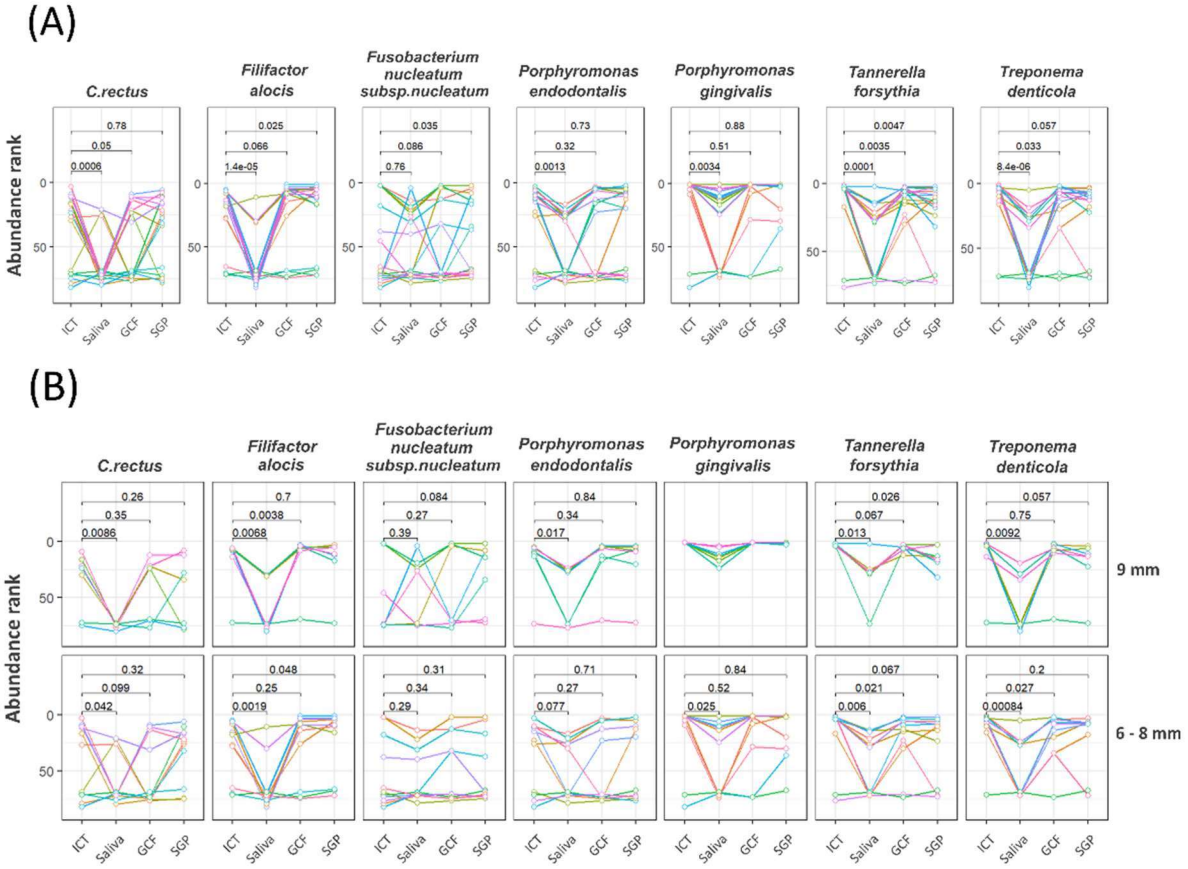

Figure 5. Abundance ranks of peri-implantitis pathogenic species among ICT, saliva, SGP and GCF.

(A) Abundance ranks of peri-implant pathogenic species (*Campylobacter rectus*, *Filifactor alocis*, *Fusobacterium nucleatum*, *Porphyromonas endodontalis*, *Porphyromonas gingivalis*, *Tannerella forsythia* and *Treponema denticola*) among the overall sample types. *P. gingivalis*, *T. forsythia*, *T. denticola*, *C. rectus*, *F. alocis* and *P. endodontalis* had significantly higher abundance ranks in ICT than in saliva. (B) Subgroup analyses of the deep- and moderate-PD groups. In the deep-PD group, *P. gingivalis* had a high abundance rank among all paired samples.

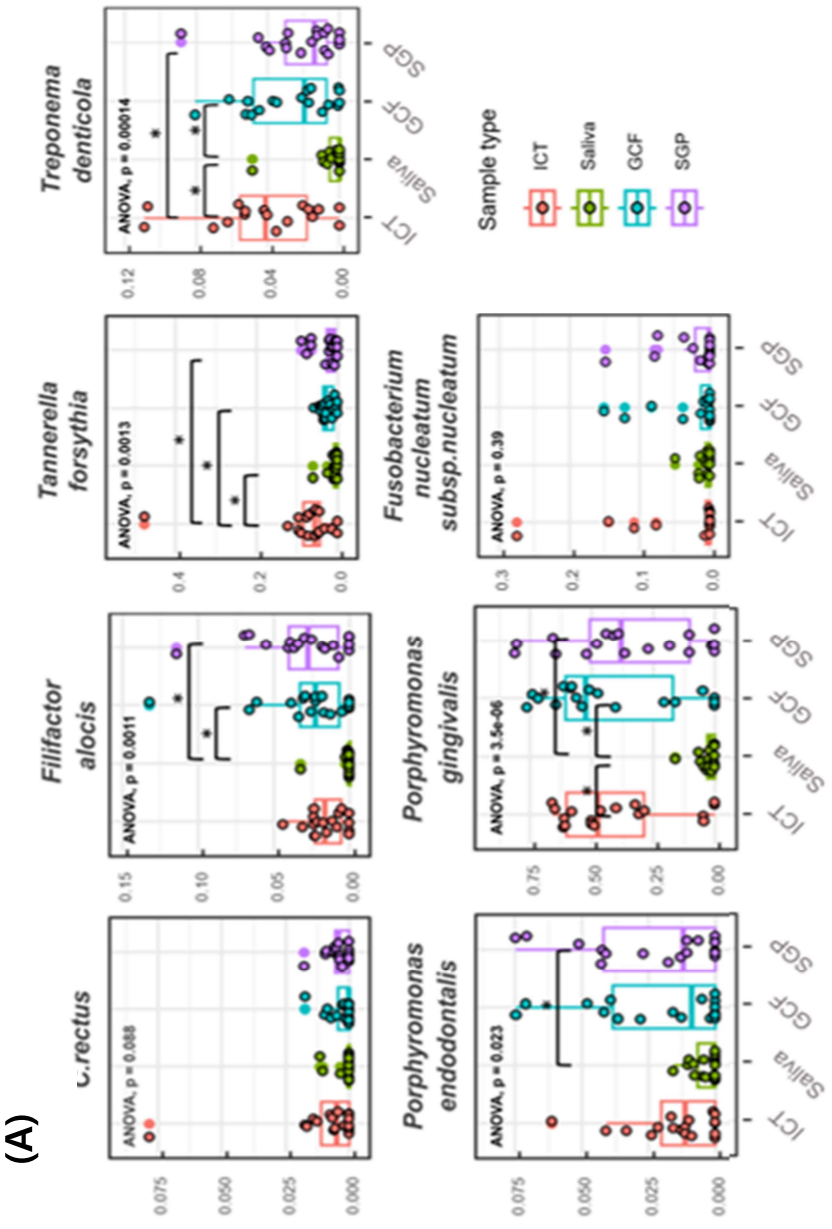

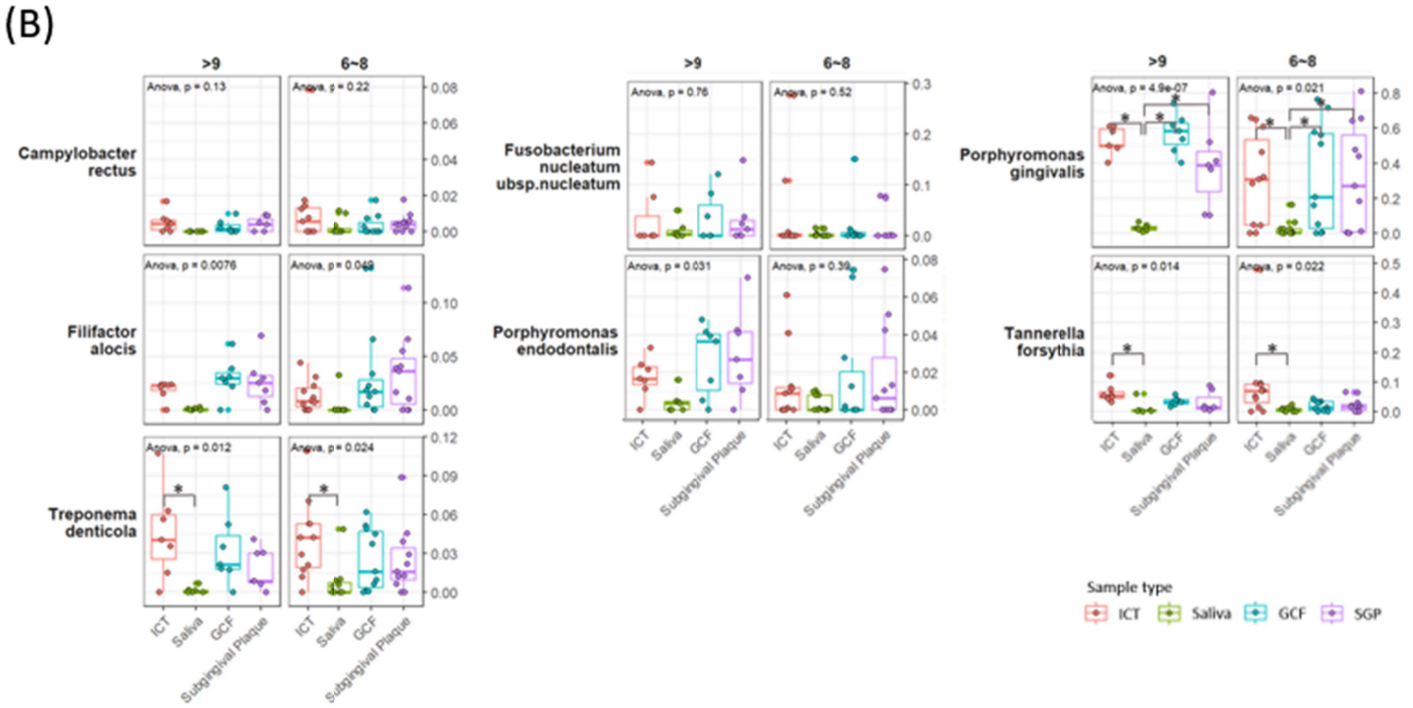

Figure 6. Relative abundances of peri-implantitis pathogenic species among ICT, saliva, SGP and GCF.

(A) The red-complex species (*P. gingivalis*, *T. forsythia* and *T. denticola*) showed significant differences in relative abundance among sample types. (B) The relative abundance of *P. gingivalis* was lower in saliva, while those of *T. forsythia* and *T. denticola* were higher in ICT, especially in the deep-PD group.

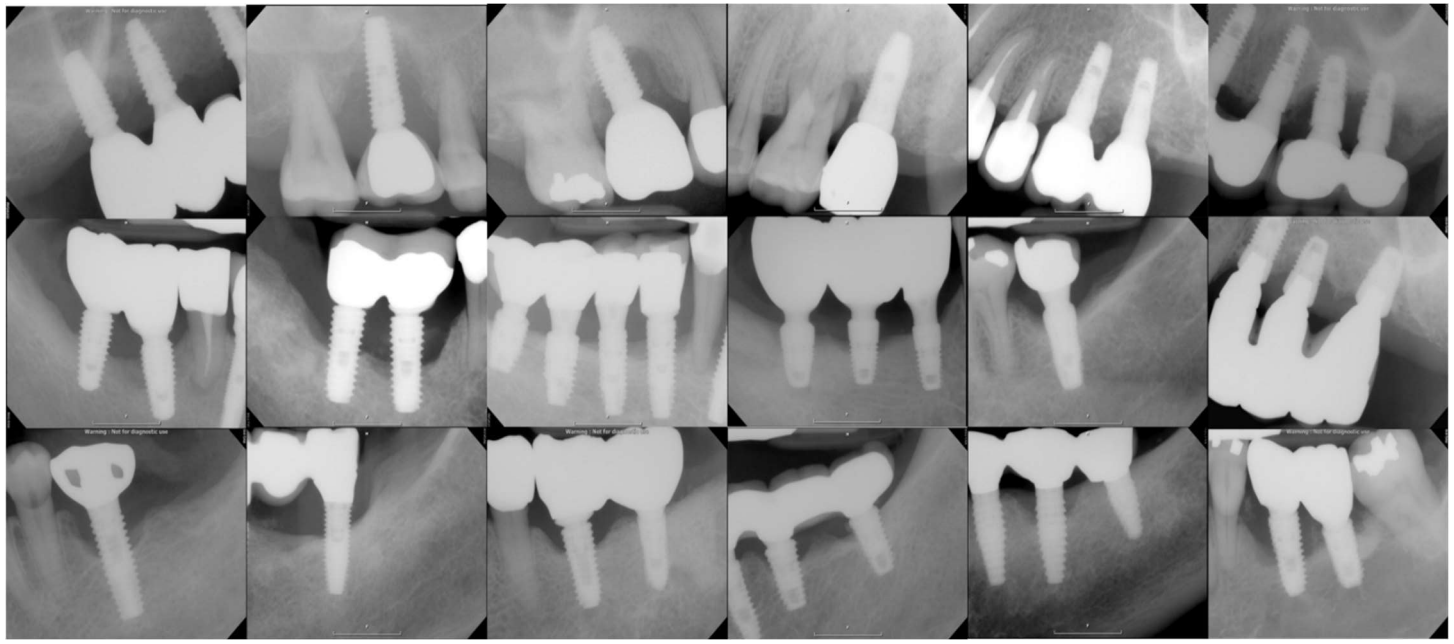

Supplementary Figure 1. Radiographs of all participants with peri-implantitis.

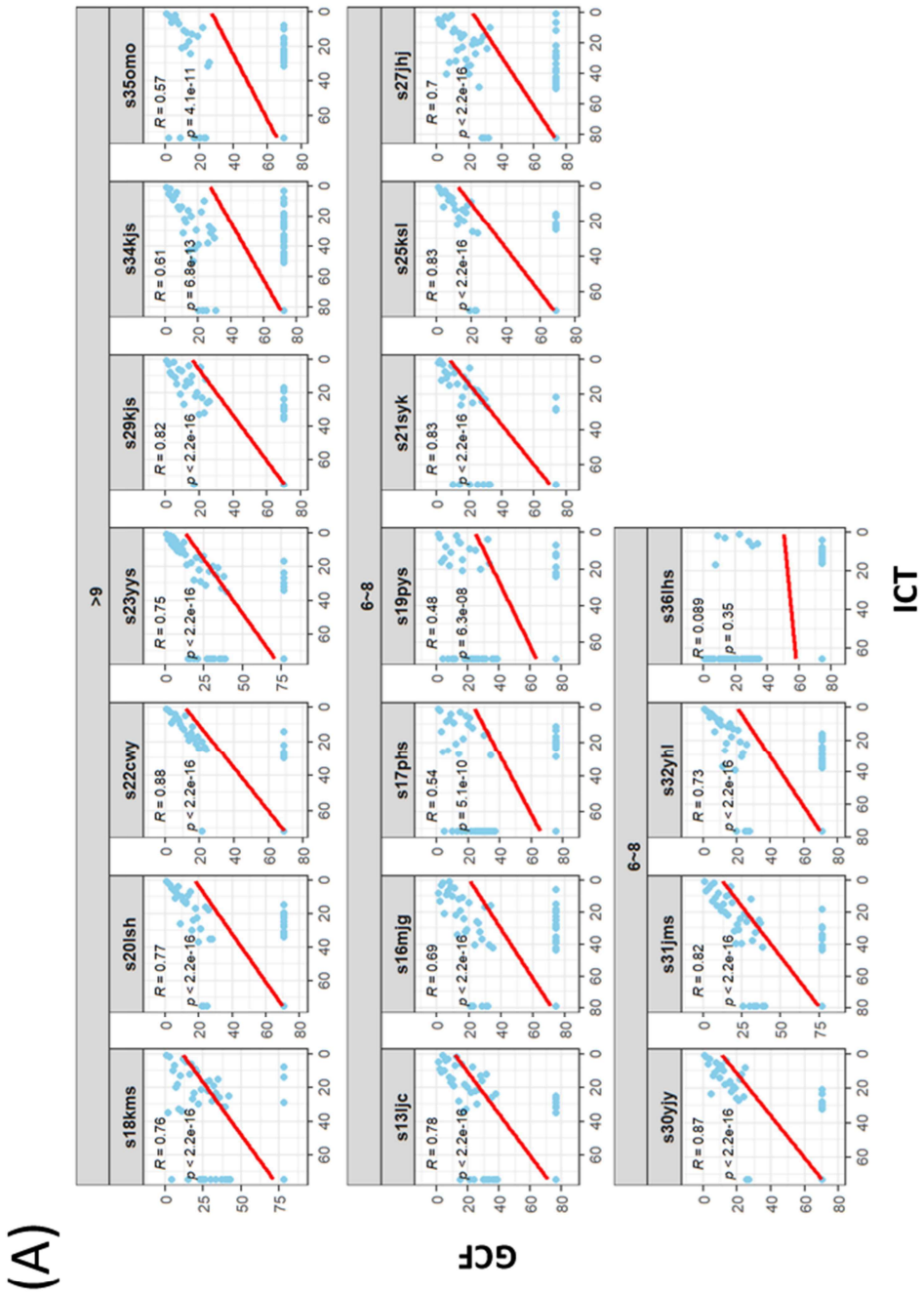

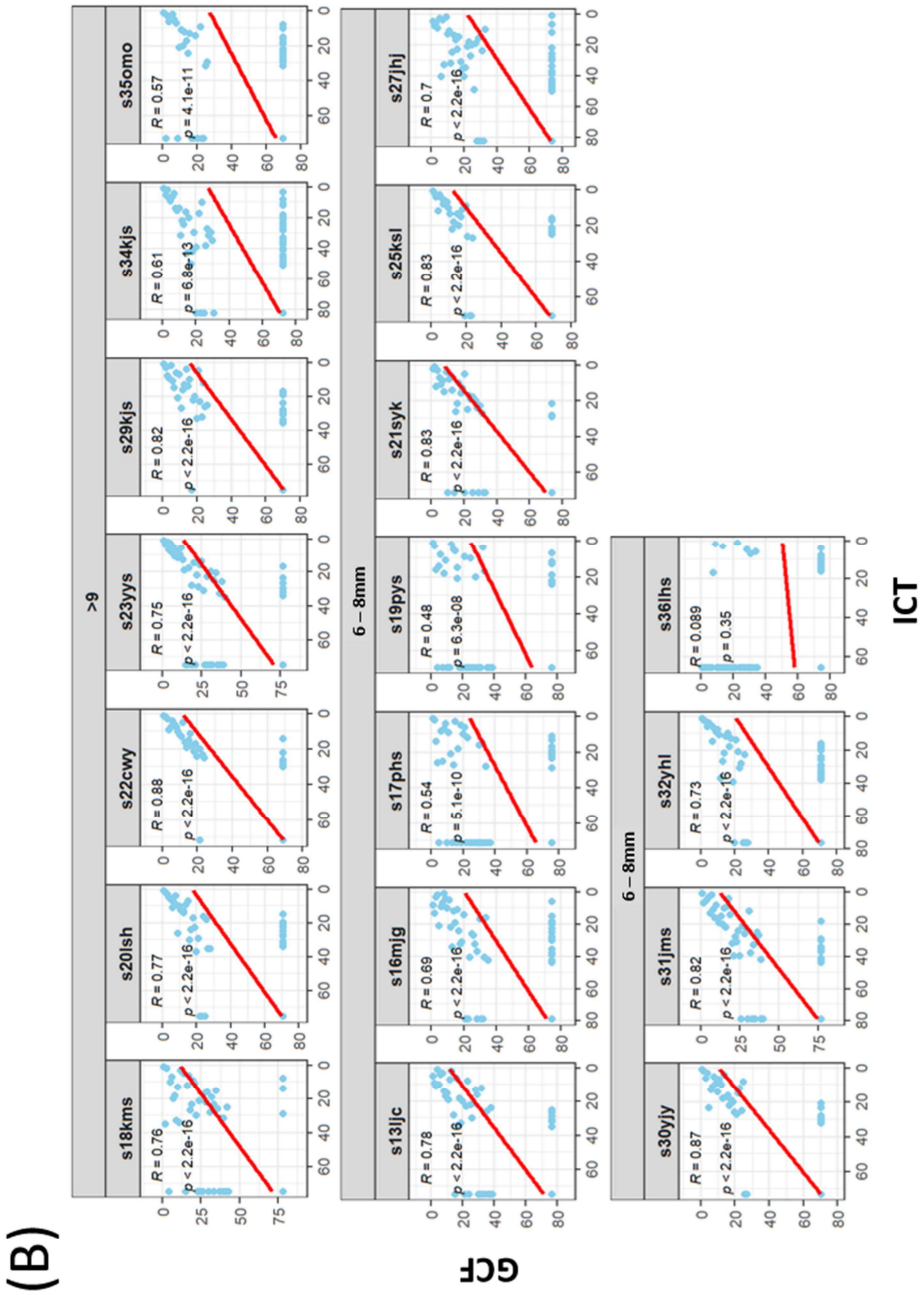

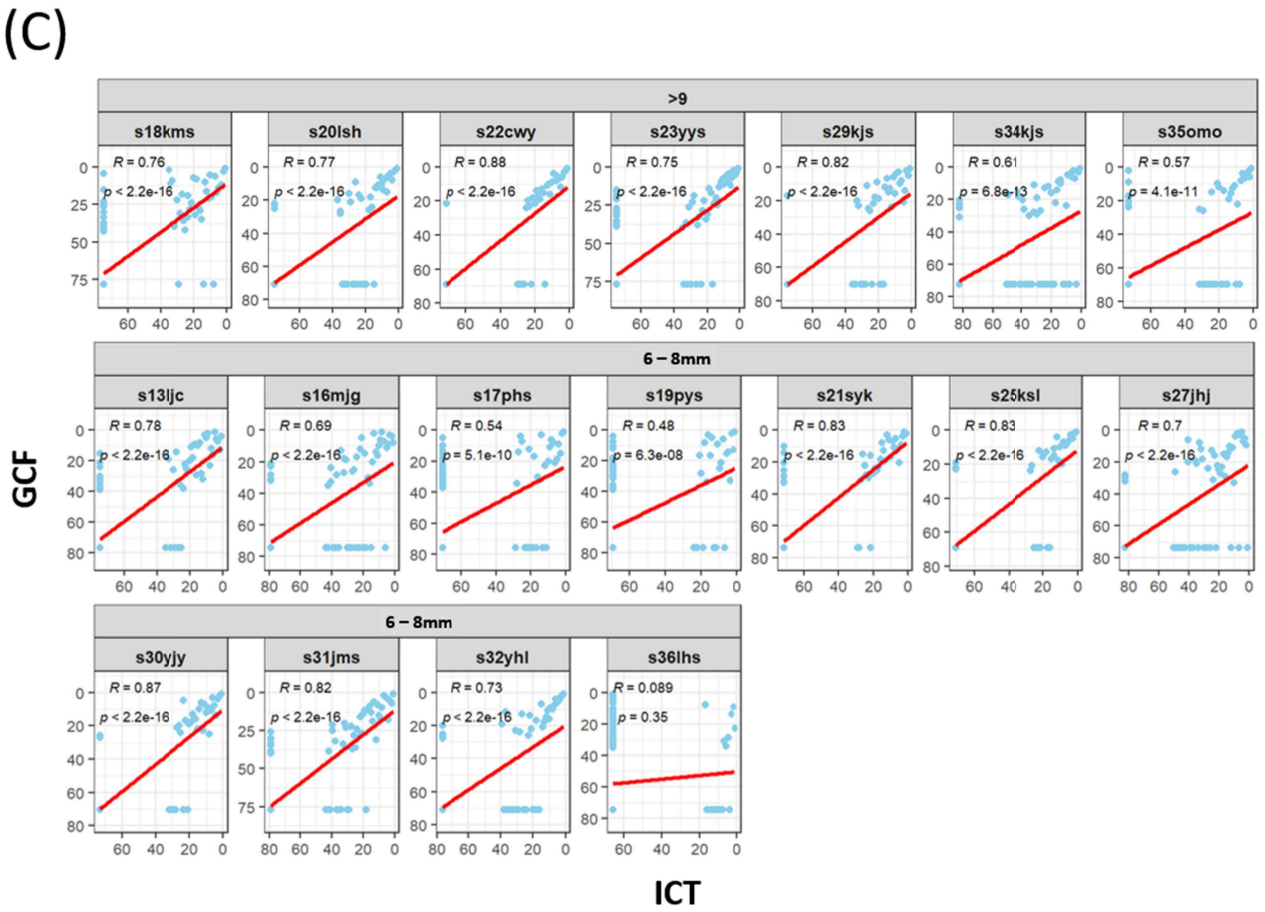

Supplementary Figure 2. Rank-abundance correlations among of microbial species between inflammatory connective tissue (ICT) and other sample types in all patients.

ICT; inflammatory connective tissue, SGP; subgingival plaque, GCF; gingival crevicular fluid

Abstract in Korean

16S RNA 시퀀싱을 이용한 임플란트 주변염 환자의 다양한 샘플 유형에 대한 마이크로바이옴 프로파일 비교

많은 연구에서 임플란트 주위염에 대한 미생물 분석을 수행했으며, 다양한 부위에서 수집한 샘플이 포함되어있다. 이에 임플란트 주위염 미생물군의 특성은 밝혀졌으나, 연구들 간의 샘플링 방법의 차이는 충분히 고려되지 않았다. 따라서, 본 연구는 임플란트 주위염이 있는 동일한 대상에서 타액, 치은열구액, 치은연하치태, 염증성 결합조직 간의 미생물 유사성을 분석하고, 임플란트 주위염 부위의 미생물 프로필을 규명하고자 한다.

본 연구는 임플란트 주위염 수술을 받는 18명의 환자로부터 타액, 치은열구액 및 치은연하치태 샘플을 수집했고, 치은을 들어올린 후 염증성 결합조직 샘플을 채취하였으며 수집된 샘플은 16S rRNA 시퀀싱을 사용하여 분석하였다.

채취한 부위는 평균 6.9mm 의 골 손실을 보였고, 가장 깊은 치주낭 깊이는 8.3mm 이였다. 알파 다양성은 염증성 결합조직, 치은열구액 및 치은연하치태 간에 유의미한 차이가 없었지만, 타액에서는 미생물 다양성이 두드러지게 나타났다. 또한, 베타 다양성은 미생물 군집 구조가 타액과 다른 샘플 간에 유의미한 차이가 없음을 보여주었다. 분류학적 분석에서는 염증성 결합조직, 치은열구액 및 치은연하치태의 미생물 프로필은 타액의 미생물 프로필과 명확히 구별할 수 있었다. 타액은 Bacteroidetes 종의 비율이 낮고 Proteobacteria 및 Actinobacteria 종의 비율이 높았으며, 특히 치주낭이 깊은 부위에서 나타났다. 피어슨 상관 분석은 염증성 결합조직과 치은열구액 및 치은연하치태 간에는 강력한 유사성을 보였지만, 염증성 결합조직과 타액 간에는 유사성을 보이지 않았다. Porphyromonas gingivalis, Tannerella forsythia, Treponema denticola, Campylobacter rectus, Filifactor alocis 및 Porphyromonas endodontalis 와 같은 병원성 종은 타액보다 ICT 에서 더 풍부했다.

결론적으로 염증성 결합조직, 치은열구액 및 치은연하치태는 유사한 미생물 프로필을 공유했지만 타액은 상당히 다른 프로필을 보였다. 이전의 샘플은 임플란트 주변

병원성 종의 풍부도가 더 높았지만 타액은 풍부도가 낮은 경향이 있었고 이러한 경향은 치주낭 깊이가 깊은 곳에서 더 두드러졌다.

핵심되는 말 : 임플란트 주위염, 16S rRNA, RNA 시퀀싱, 마이크로바이옴